

PHOTOPRODUCTION OF ETA AND ETAPRIME MESONS ON THE NUCLEON

LOTHAR TIATOR

*Institut für Kernphysik, Universität Mainz
D-55099 Mainz, Germany
tiator@kph.uni-mainz.de*

The isobar models η -MAID and η' -MAID have been used to analyze new data on quasi-free η photoproduction on the deuteron from Bonn and recent η' data on the proton from Jlab. In η photoproduction on the neutron a bump around $W = 1700$ MeV was observed which could possibly arise from a narrow P_{11} state that is discussed as a non-strange member of the Θ^+ antidecuplet. In η' photoproduction on the proton resonance contributions are found that can be attributed to missing resonances in the energy region around $W = 1900$ MeV.

Keywords: Eta Meson; Photoproduction; Nucleon Resonances.

PACS numbers: 13.60.Le, 14.20.Gk, 25.20.Lj, 25.30.Rw

1. Introduction

In recent experiments of eta photoproduction on the deuteron at GRAAL¹ and at CB-TAPS-ELSA² an enhanced cross section has been observed in the neutron channel around $W = 1700$ MeV, which is not visible in eta photoproduction on the proton target. In 1997, Diakonov, Petrov and Polyakov had predicted an exotic anti-decuplet of baryons within the chiral soliton model³. Besides the famous $\Theta^+(1530)$, they also predicted a non-strange member $N(1710)$, which could have been identified with the $P_{11}(1710)$ state listed in the particle data tables⁵. Furthermore, this state was predicted with a much stronger coupling to the ηN than to the πN channel. After the first pentaquark signals had been reported⁶, in a new partial wave analysis Arndt et al.⁷ reported about two possible non-strange candidates with masses 1680 MeV and 1730 MeV and widths smaller than 30 MeV. Before, Polyakov and Rathke⁴ had shown that within their model, the non-strange member of the antidecuplet around 1700 MeV should couple much stronger electromagnetically to the neutron than to the proton. In this respect the new observations received some attractions and explanations with pentaquark states have been searched. However, very different to the Θ^+ signals that were reported as extremely narrow peaks of the order of and even below 1 MeV, the bump in eta photoproduction is quite broad and looks more like a typical nucleon resonance structure with a width of the order of 100 MeV.

Surprisingly, the isobar model EtaMaid2001⁸ which was only fitted to proton

2 *Lothar Tiator*

data available in 2001, describes this bump structure very well. The reason is that the $D_{15}(1675)$ resonance came out of this fit with an unusually large ηN branching ratio, strongly violating $SU(3)$ symmetry bounds⁹. Already from pion photoproduction and also from the simple quark model, the D_{15} resonance is well known as a resonance that couples much stronger to the neutron than to the proton. As an alternative to the strong D_{15} model, in our more recent isobar analysis (EtaMaid2003) we have found that a modification of the nonresonant background, however, would modify the eta branching very strongly. In Tables 1 and 2 it is shown that some higher resonances (and in particular the D_{15}) almost disappear if the standard treatment of t -channel vector meson exchange with single poles is replaced by Regge trajectories. Such a reggeization is definitely required at very large energies of a few GeV, but at the rather low energies of $E_\gamma \approx 1$ GeV, where the bump occurs, Regge trajectories are usually not seriously considered.

2. Isobar models for η and η' photoproduction

The isobar models η -MAID and η' -MAID are similar to the unitary isobar model MAID. They are constructed with a nonresonant background of nucleon Born terms and t -channel vector meson exchange, plus a number of s -channel nucleon resonance excitations,

$$t_{\gamma,\eta}^\alpha = v_{\gamma,\eta}^\alpha(Born + \omega, \rho) + t_{\gamma,\eta}^\alpha(Resonances). \quad (1)$$

The nonresonant background contains the usual Born terms and vector meson exchange contributions. It is obtained by evaluating the Feynman diagrams derived from an effective Lagrangian. The Born terms are evaluated in the standard way with pseudoscalar coupling, and the details can be found in Ref. 8. In the reggeized model, however, we do not include the Born terms. The reason is that the correct treatment for the u -channel nucleon exchange, together with the reggeized t -channel vector meson exchanges, requires to also introduce the nucleon Regge trajectories. Because of the lack of high energy data at backward angles, it is currently difficult to determine this u -channel contribution. Since the coupling constants $g_{\eta NN}$ and $g_{\eta' NN}$ are small, the difference caused by the absence of the Born terms is negligible at low energies.

For each partial wave α the resonance excitation is parameterized with standard Breit-Wigner functions with energy dependent widths,

$$t_{\gamma,\eta}^\alpha(R; \lambda) = \tilde{A}_\lambda \frac{\Gamma_{tot} W_R}{W_R^2 - W^2 - iW_R \Gamma_{tot}} f_{\eta N}(W) C_{\eta N} \zeta_{\eta N}, \quad (2)$$

where a hadronic phase is introduced, $\zeta_{\eta N} = \pm 1$, a relative sign between the $N^* \rightarrow \eta N$ and the $N^* \rightarrow \pi N$ couplings. For a few states the relative phases are well determined and can be found in the Particle Data Tables, for most of the states it can be used as a free parameter in our partial wave (pw) analysis. The principal fit parameters of our pw analysis are the resonance masses $W_R \equiv M^*$, the total widths $\Gamma_R = \Gamma_{tot}(W_R)$, the branching ratios $\beta_{\eta N} = \Gamma_{\eta N}(W_R)/\Gamma_R$ and the photon

couplings $\tilde{A}_\lambda = \{A_{1/2}, A_{3/2}\}$. However, we fix those parameters, where reliable results are given by PDG, see Tables 1 and 2.

The total width Γ_{tot} in Eq. (2) is the sum of $\Gamma_{\eta N}$, the single-pion decay width $\Gamma_{\pi N}$, and the rest, for which we assume dominance of the two-pion decay channels,

$$\Gamma_{\text{tot}}(W) = \Gamma_{\eta N}(W) + \Gamma_{\pi N}(W) + \Gamma_{\pi\pi N}(W). \quad (3)$$

The details of the parametrization of the energy-dependent widths and the vertex function $f_{\eta N}(W)$ can be found in Refs. 8, 10.

3. Results

3.1. η photoproduction results on protons and neutrons

In this section, we present the η photoproduction results from the reggeized model as well as the standard η -MAID model with vector meson pole contributions. In the reggeized model, we replace the t -channel ρ and ω exchanges used in η -MAID by the Regge trajectories while keeping the same N^* contributions. Both models are fitted to photoproduction data of cross sections from TAPS¹¹, GRAAL¹², and CLAS¹³ as well as polarized beam asymmetries from GRAAL¹⁴.

Table 1. Parameters of nucleon resonances from EtaMaid2003 with standard vector meson poles, model (I). The masses and widths are given in MeV, $\beta_{\eta N}$ is the branching ratio for the eta decay channel and $\zeta_{\eta N}$ the relative sign between the $N^* \rightarrow \eta N$ and the $N^* \rightarrow \pi N$ couplings. The photon couplings to the proton and neutron target for helicity $\lambda = 1/2$ and $3/2$ are given in units of $10^{-3}/\sqrt{GeV}$. The underlined parameters are fixed and are taken from PDG2004⁵. The asterisk for $nA_{1/2}$ of the $S_{11}(1535)$ denotes a fixed n/p ratio obtained from the experiment¹⁵.

N^*	Mass	Width	$\beta_{\eta N}$	$\zeta_{\eta N}$	$pA_{1/2}$	$pA_{3/2}$	$nA_{1/2}$	$nA_{3/2}$
$D_{13}(1520)$	<u>1520</u>	<u>120</u>	0.05%	+1	-39	<u>166</u>	<u>-59</u>	<u>-139</u>
$S_{11}(1535)$	1545	203	<u>50%</u>	+1	125	-	-102*	-
$S_{11}(1650)$	1640	130	10%	-1	73	-	-59	-
$D_{15}(1675)$	1682	<u>150</u>	17%	-1	17	24	<u>-43</u>	<u>-58</u>
$F_{15}(1680)$	1670	<u>130</u>	0.04%	+1	-9	145	<u>29</u>	<u>-33</u>
$D_{13}(1700)$	<u>1700</u>	<u>100</u>	0.7%	-1	<u>-18</u>	<u>-2</u>	<u>0</u>	<u>-3</u>
$P_{11}(1710)$	1725	<u>100</u>	26%	+1	22	-	<u>-2</u>	-
$P_{13}(1720)$	<u>1720</u>	<u>150</u>	6.6%	-1	<u>18</u>	<u>-19</u>	<u>1</u>	<u>-29</u>

In Fig. 1 we compare our results with published data (upper panels) and with the preliminary results of the CB-TAPS-ELSA experiment (lower panels) for both EtaMaid2003 versions. The model using standard vector meson poles, similar to the EtaMaid2001 model, produces a bump in the neutron cross section, whereas the model with vector meson Regge trajectories shows similar structures for proton and neutron cross sections and leads therefore to a flat neutron to proton ratio.

The problem with our model (I) is the unusually large ηN branching ratio of 17% for the D_{15} resonance, which strongly violates $SU(3)$, where an upper limit

4 Lothar Tiator

Table 2. Parameters of nucleon resonances from EtaMaid2003 with reggeized vector mesons, model (II). Notation as in Table 1.

N^*	Mass	Width	$\beta_{\eta N}$	$\zeta_{\eta N}$	${}_p A_{1/2}$	${}_p A_{3/2}$	${}_n A_{1/2}$	${}_n A_{3/2}$
$D_{13}(1520)$	1520	120	0.04%	+1	-24	166	-59	-139
$S_{11}(1535)$	1521	118	50%	+1	80	-	-65*	-
$S_{11}(1650)$	1635	120	16%	-1	46	-	-38	-
$D_{15}(1675)$	1665	150	0.7%	+1	19	15	-43	-58
$F_{15}(1680)$	1670	130	0.003%	+1	-15	133	29	-33
$D_{13}(1700)$	1700	100	0.025%	-1	-18	-2	0	-3
$P_{11}(1710)$	1700	100	26%	-1	9	-	-2	-
$P_{13}(1720)$	1720	150	4%	+1	18	-19	1	-29

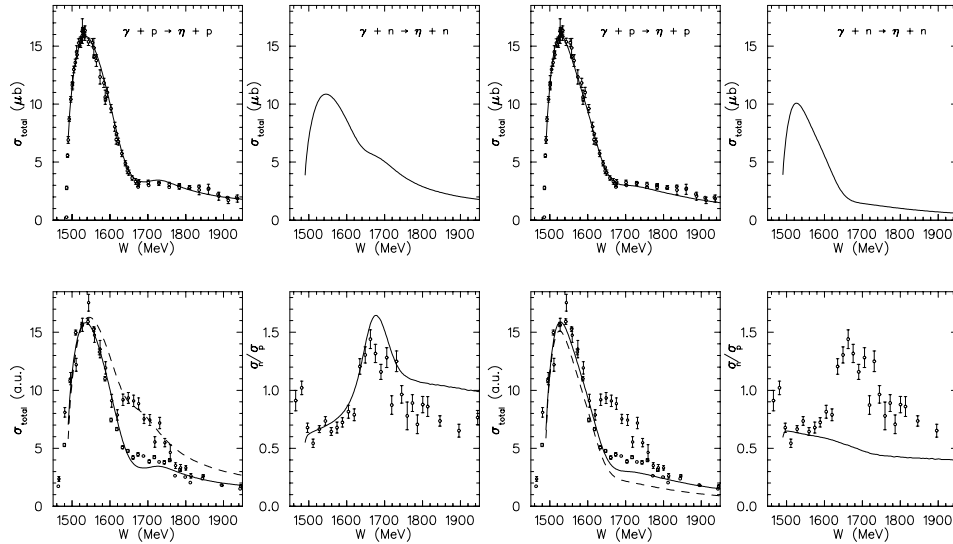


Fig. 1. Total cross sections for eta photoproduction on proton and neutron (left: Maid2003 with standard vector meson poles, right: Maid2003 with reggeized vector mesons). In the upper row the calculations are compared to published data on the proton target from MAMI¹¹ (in larger energy bins), GRAAL¹⁶ (without the five largest energy points), CLAS¹³ and CB-ELSA¹⁷. In the lower row the calculations are compared to preliminary data of CB-TAPS-ELSA², shown in arbitrary units.

Table 3. Mass, total width, ηN branching ratio and photon helicity couplings in units of $(10^{-3}/\sqrt{GeV})$ for the P_{11} pentaquark state in our calculation.

M^* (MeV)	Γ_{tot} (MeV)	$\Gamma_{\eta N}/\Gamma_{tot}$	$A_{1/2}(p)$	$A_{1/2}(n)$
1675	10	40%	10	30

of 2.5% has been evaluated⁹. Furthermore, it may also be in conflict with single and double pion photoproduction data on the neutron as well as with the hadronic

π, η reactions, that are the more standard sources for branching ratios. However, all those data are not good enough to draw definite conclusions. On the other side, the reggeized model (II), which does not require a large D_{15} coupling in order to explain the cross section and beam asymmetry data cannot describe the bump structure in the neutron data. This is drastically shown in the neutron to proton ratio in Fig. 1 (last panel). Alternatively, we have studied the excitation of a narrow P_{11}

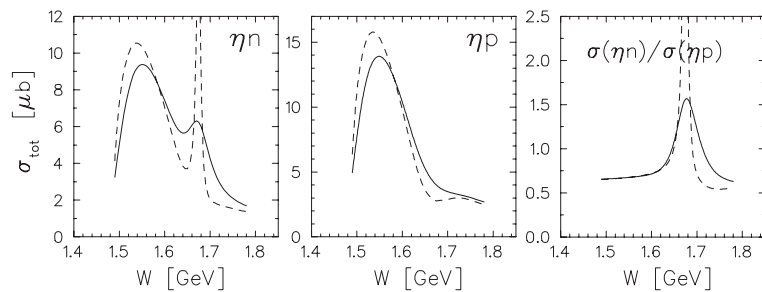


Fig. 2. Eta photoproduction with a pentaquark state with properties given in Table 3. The dashed lines show the production on a free nucleon and the solid lines on a quasi-free nucleon of a deuteron target.

pentaquark state in the quasi-free eta photoproduction off the deuteron. Already Diakonov et al.³ in a chiral soliton model and Arndt et al.⁷ in a modified partial wave analysis had reported about a possible P_{11} state in the region around 1680 – 1730 MeV with a width smaller than 30 MeV, that should couple quite strongly to the ηN channel. Furthermore, Polyakov and Rathke⁴ have shown that the e.m. transition moment of the neutron should be much larger than for the proton, with a ratio of $\mu_{nN^*}/\mu_{pN^*} \gtrsim 3$. Based on these properties we have included this state as a $P_{11}(1675)$ resonance in our isobar model with parameters given in Table 3 and have calculated the cross sections for both a free proton and a free neutron target. The total cross sections can be seen in Fig. 2, where for the neutron this state pops out of the background as a sharp resonance, while it is hidden in the background for the proton target. The huge difference can be understood from the fact, that the e.m. moments or couplings enter quadratically in the cross sections, thus giving a ratio of one order of magnitude.

However, such a sharp resonance would not show up in an experiment on a bound neutron in a deuteron target. Due to Fermi motion, the sharp resonance state becomes broadened and gets a shape similar to an ordinary nucleon resonance with a width of around 100 MeV. The solid line in Fig. 2 shows a calculation in the spectator-nucleon approach¹⁸. Further corrections of NN and ηNN final state interaction are expected to be small¹⁸.

While both reaction mechanisms give similar results for the total cross section, due to the different orbital momentum of the D_{15} and P_{11} resonances, they will show up with different angular distributions. In Fig. 3 we show our calculations for

6 *Lothar Tiator*

a neutron at $W = 1668$ MeV for a) the strong D_{15} model, b) the narrow P_{11} model with a phase $\zeta_{\eta N} = +1$ and c) the narrow P_{11} model with a phase $\zeta_{\eta N} = -1$. For all three cases we compare the calculation for a free neutron with the quasi-free

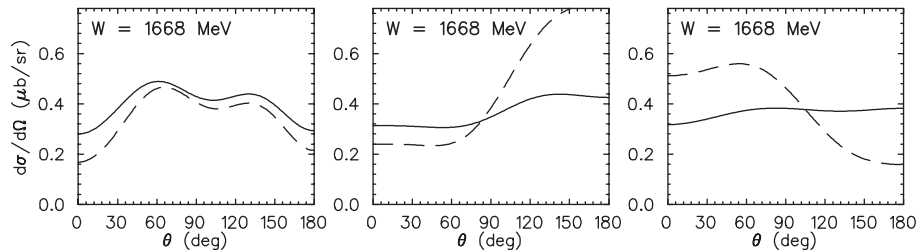


Fig. 3. Differential cross section for eta photoproduction on the neutron at $W = 1668$ MeV. From left to right, the first panel shows the result of η -Maid2003 with standard vector meson poles and a strong $D_{15}(1675)$ resonance, the second panel shows the result with the reggeized model and a narrow $P_{11}(1675)$ resonance with a hadronic phase $\zeta_{\eta N} = +1$, the third panel is similar to the second but with a negative hadronic phase. The dashed lines are for a free neutron target and the solid lines for a quasi-free neutron of a deuteron target. The cross section on a quasi-free neutron refers to the so-called effective γN^* system, where the initial nucleon is assumed to be at rest in the deuteron. A more detailed description of this system can be found in Ref. 11.

calculation on the deuteron. In case a) the averaging over the spectator nucleon due to Fermi motion gives only a small effect, whereas in the cases b) and c) with the narrow pentaquark state the Fermi smearing is very large, in particular at the chosen energy very close to the resonance peak. In the angular distribution the hadronic phase becomes very important, since the P_{11} partial wave interferes with other partial waves like the S_{11} . In the total cross section it can only interfere with other contributions in the same partial wave, e.g. from the background, and the difference can hardly be seen.

3.2. η' photoproduction results on protons

The experimental data base for η' photoproduction is still rather limited. Besides the total cross section data measured decades ago at DESY, the only modern data were obtained at SAPHIR-ELSA¹⁹ and very recently at JLab/CLAS²⁰. Further data for differential cross sections have been taken at CB-ELSA which can be expected to come out soon.

The isobar model η' -MAID is conceptual very similar to the η -MAID. The vector meson couplings used in the t -channel exchanges are well determined: The photon couplings can be obtained from the electromagnetic decay widths of $\eta' \rightarrow \rho\gamma$ and $\eta' \rightarrow \omega\gamma$ and for the strong couplings the same values as in η photoproduction are used. Furthermore, we neglect the Born terms as in the case of η photoproduction. Therefore, the background contributions are completely fixed and only the resonance parameters are varied to fit the data.

In our fit to the η' data we use as free parameters the resonance mass and

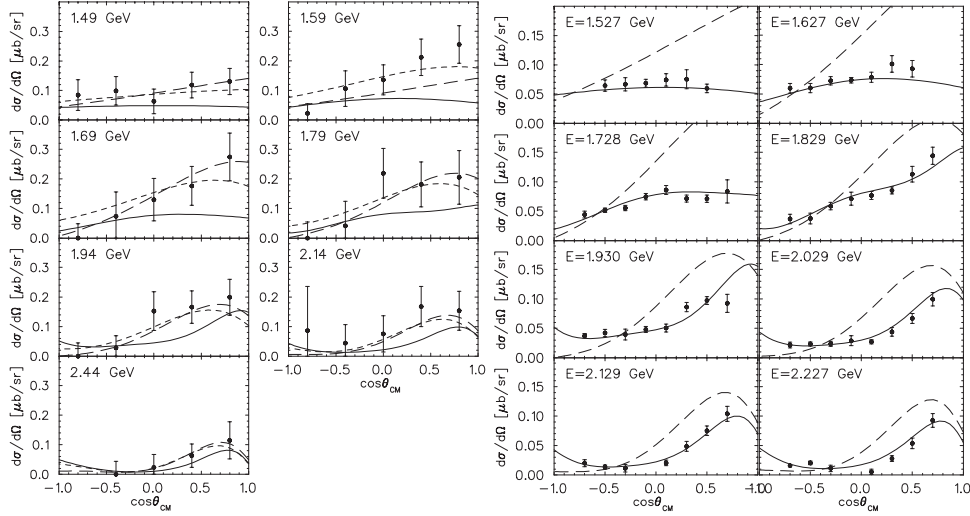


Fig. 4. Etaprime photoproduction on the proton. On the left we show the SAPHIR data of 1998 and on the right the CLAS data of 2006. The dotted lines and the dashed lines show our one(S_{11})- and two-resonance(S_{11}, P_{11}) fits from 2003 to the SAPHIR data only. The solid lines are our new fits to the CLAS data including four resonances $S_{11}, P_{13}, P_{11}, D_{13}$ as listed in Table 4.

width as well as the photon couplings $A_{1/2}$ and $A_{3/2}$. The also unknown branching ratios into the $\eta'N$ channel cannot be fitted simultaneously. Therefore, we only determine effective $p(\gamma, \eta')p$ couplings for both helicity states, $\chi_{1/2} = \sqrt{\beta_{\eta'N}} A_{1/2}$ and $\chi_{3/2} = \sqrt{\beta_{\eta'N}} A_{3/2}$. The results of our fit to the new CLAS data are given in Table 4.

Table 4. Mass, total width, and effective $p(\gamma, \eta')p$ couplings for total helicity 1/2 and 3/2 in units of ($10^{-3}/\sqrt{GeV}$) as defined in the text.

resonance	M^* (MeV)	Γ_{tot} (MeV)	$\chi_{1/2}$	$\chi_{3/2}$
S_{11}	1904	527	15.7	–
P_{13}	1926	146	-1.5	1.0
P_{11}	2083	51	2.5	–
D_{13}	2100	91	6.5	-6.5

From our previous fit to the SAPHIR data we concluded three solutions with a reggeized vector meson background and a) an $S_{11}(1959)$ resonance, b) an $S_{11}(1932)$ and a $P_{11}(1951)$ and c) an $S_{11}(1933)$ and a $P_{13}(1954)$. All of them give similar χ^2 with the old Bonn data but fail to describe the new CLAS data. Therefore, we performed a new fit only to the CLAS data, shown in Fig. 4 as the solid line, that includes four nucleon resonances, S_{11}, P_{13}, P_{11} and D_{13} . The fitted parameters of these states are given in Table 4. The S_{11} and P_{13} states cannot be found in the Particle Data Tables and could be identified with the missing resonances that are

8 *Lothar Tiator*

claimed in many quark model calculations, e.g. Refs. 21, 22, 23. The P_{11} and D_{13} states around $W = 2100$ MeV can be identified with the listed states $P_{11}(2100)$ and $D_{13}(2080)$. This data is also well fitted within the relativistic meson-exchange models of Sibirtsev²⁴ and Nakayama, Haberzettl²⁵, including also the hadronic reaction $pp \rightarrow pp\eta'$. Besides the sub-threshold resonances $S_{11}(1535)$, $P_{11}(1710)$, $D_{13}(1780)$ which contribute to the background, the fit to the data also finds resonant contributions of $P_{13}(1940)$ and $D_{13}(2090)$, see Ref. 20. Obviously, with only differential cross section data many solutions with different resonances are possible and no definite conclusions can be drawn at this stage.

4. Summary and conclusions

In this paper we have presented a new partial wave analysis with recent data on η and η' photoproduction. The data give rise to interesting speculations about a narrow P_{11} resonance in $n(\gamma, \eta)n$ and missing resonances in $p(\gamma, \eta')p$. However, these solutions are not unique. Further experimental investigations are necessary in order to clarify the situations. Precise angular distributions of quasi-free eta photoproduction on the deuteron could solve the question about the pentaquark. In the case of etaprime production, polarization data, e.g. beam asymmetry could be very helpful to better determine the partial wave contributions in this reaction.

Acknowledgments

I would like to thank Prof. B. Krusche and I. Jaegle of the CB-ELSA collaboration and Dr. M. Dugger from the JLab/CLAS collaboration for kindly sharing their data before publication. In particular I am also grateful to Dr. A. Fix for his help in the quasi-free eta photoproduction calculations on the deuteron. This work was supported by the Deutsche Forschungsgemeinschaft (SFB 443).

References

1. V. Kouznetsov et al., Proc. of the NSTAR2004 workshop, Grenoble, France, 2004, World Scientific 2004, p. 197.
2. I. Jaegle, Proc. of the NSTAR2005 workshop, Tallahassee, FL, USA, 2005, World Scientific 2006, p. 340 and I. Jaegle, private communication.
3. D. Diakonov, V. Petrov, and M.V. Polyakov, Z. Phys. A 359, 305 (1997).
4. M.V. Polyakov and A. Rathke, Eur. Phys. J. A 18, 691 (2003) and M.V. Polyakov, private communication.
5. S. Eidelman *et al.*, Phys. Lett. B 592, 1 (2004).
6. T. Nakano et al., Phys. Rev. Lett. 91, 012002 (2003).
7. R.A. Arndt, Ya.I. Azimov, M.V. Polyakov, I.I. Strakovsky and R.L. Workman, Phys. Rev. C 69, 035208 (2004).
8. W.-T. Chiang, S.N. Yang, L. Tiator and D. Drechsel, Nucl. Phys. A 700, 429 (2002).
9. V. Guzey and M.V. Polyakov, hep-ph/0512355 and M.V. Polyakov, private communication.
10. W.-T. Chiang, S.N. Yang, L. Tiator, M. Vanderhaeghen and D. Drechsel, Phys. Rev. C 68, 045202 (2003).

11. B. Krusche *et al.*, Phys. Rev. Lett. 74, 3736 (1995).
12. F. Renard *et al.*, Phys. Lett. B 528, 215 (2002).
13. M. Dugger *et al.*, Phys. Rev. Lett. 89, 222002 (2002); 89 (2002) 249904(E).
14. J. Ajaka *et al.*, Phys. Rev. Lett. 81, 1797 (1998).
15. B. Krusche *et al.*, Phys. Lett. B 358, 40 (1995).
16. F. Renard *et al.*, Phys. Lett. B 528, 215 (2002).
17. V. Crede *et al.*, Phys. Rev. Lett. 94, 012004 (2005).
18. A. Fix and H. Arenhövel, Z. Phys. A359, 427 (1997) and A. Fix, priv. comm.
19. R. Plötzke *et al.*, Phys. Lett. B 444, 555 (1998).
20. M. Dugger *et al.*, Phys. Rev. Lett. 96, 062001 (2006).
21. S. Capstick and N. Isgur, Phys. Rev. D 34, 2809 (1986).
22. M. Ferraris, M.M. Giannini, M. Pizzo, E. Santopinto and L. Tiator, Phys. Lett. B 364, 231 (1995); M.M. Giannini, E. Santopinto and A. Vassallo, Proc. NSTAR2002, Pittsburgh, PA, USA, World Scientific, Singapore, 2003, p. 296 (nucl-th/0302019).
23. U. Loring, B.C. Metsch, H.R. Petry, Eur. Phys. J. A 10, 395 (2001).
24. A. Sibirtsev, Ch. Elster, S. Krewald and J. Speth, AIP Conf. Proc. 717, 837 (2004).
25. K. Nakayama and H. Haberzettl, Phys. Rev. C 69, 065212 (2004).